ELSEVIER

Biochimica et Biophysica Acta 1563 (2002) 53–63

BIOCHIMICA ET BIOPHYSICA ACTA
BBA

www.bba-direct.com

Conformational states of the cell-penetrating peptide penetratin when interacting with phospholipid vesicles: effects of surface charge and peptide concentration

Mazin Magzoub, L.E. Göran Eriksson, Astrid Gräslund*

Department of Biochemistry and Biophysics, The Arrhenius Laboratories, Stockholm University, Svante Arrhenius vag 10-12, S-106 91 Stockholm, Sweden

Received 21 November 2001; received in revised form 8 February 2002; accepted 20 February 2002

Abstract

The most commonly studied of the cell-penetrating peptides (CPP) is "penetratin" (pAntp), which functions as a carrier (vector), even for large hydrophilic (cargo) molecules. pAntp originates from the third helix of the Antennapedia homeodomain protein. The peptide is known to interact with negatively charged phospholipid vesicles, which leads to induction of secondary structure. In the present study, circular dichroism (CD) spectroscopy has been used to characterize the different secondary structures induced upon interaction with small unilamellar vesicles (SUVs) from mixtures of zwitterionic 1-palmitoyl-2-oleoyl-phosphatidylcholine (POPC) and negatively charged 1-palmitoyl-2-oleoyl-phosphatidylglycerol (POPG). The interaction was monitored using an electron paramagnetic resonance (EPR) spin probe attached to the peptide, and the intrinsic fluorophore (tryptophan). We measured the secondary structure as a function of surface charge density, total lipid-to-peptide (L/P) molar ratio, and salt concentration, for completely bound peptide. With vesicles from POPG/POPC in a molar ratio below 30:70, at a high L/P, the peptide adopts a mainly helical conformation. Increasing the charge density, at the same L/P, promotes a higher degree of β-structure. At a fixed charge density, reducing the L/P also results in an $\alpha \rightarrow \beta$ structure conversion. Hence, low membrane surface charge density and low pAntp concentration both favor a mainly helical conformation, while high charge density and pAntp concentration promote a dominating β-structure. We conclude that pAntp, when residing at the surface of a membrane, is chameleon-like in terms of its induced structure. © 2002 Published by Elsevier Science B.V.

Keywords: Penetratin; Phospholipid vesicle; Surface charge; Interaction; Secondary structure

1. Introduction

Cell-penetrating peptide (CPP) is a term used to describe a number of natural and synthetic peptides, which are water-soluble but are still able to translocate various cell membranes with high efficiency and low lytic activity. This transport is non-endocytotic and non-cell-type specific [1,2]. When covalently linked to a "cargo", including polypeptides and oligonucleotides, many times their own molecular mass, CPPs still retain their translocating ability. All these factors have led to CPPs, also known as "Trojan" peptides [1], being used as vectors for the delivery of hydrophilic biomolecules and drugs into cytoplasmic and nuclear compartments of cells, both in vivo and in vitro [1,2].

Examples of CPPs are so-called Tat-derived peptides, as well as peptides based on signal sequences, but the most common are those with sequences derived from the homeodomains of certain transcription factors. Homeodomain (homeobox) proteins belong to a class of transcription factors involved in multiple morphological processes [3]. The first reported example of a homeodomain-derived translocating peptide is "penetratin", which is also the most widely studied of all the CPPs. Penetratin (denoted pAntp[1]) has a sequence corresponding to the 16 residues of the third α-helix (residues 43 to 58: RQIKIWFQNRRMKWKK) of

Abbreviations: pAntp, penetratin, Antennapedia homeodomain derived transport peptide; CPP, cell-penetrating peptide; CD, circular dichroism; POPC, 1-palmitoyl-2-oleoyl-phosphatidylcholine; POPG, 1-palmitoyl-2-oleoyl-phosphatidylglycerol; L/P, total lipid-to-peptide (pAntp) molar ratio; EPR, electron paramagnetic resonance; MTS-SL, (1-oxyl-2,2,5,5-tetramethyl-pyrroline-3-methyl) methanethiosulfonate spin label; SL-pAntp, cys(-1)-pAntp spin labeled by the MTS-SL reagent; SUVs, small unilamellar vesicles

* Corresponding author. Tel.: +46-8-162450; fax: +46-8-155597.
E-mail address: astrid@dbb.su.se (A. Gräslund).

0005-2736/02/$ - see front matter © 2002 Published by Elsevier Science B.V.
PII: S0005-2736(02)00373-5

the Antennapedia homeodomain of *Drosophila* [4–6]. This third helix was found to be responsible not only for the interaction with DNA by binding specifically to cognate sites in the genome, but also for the translocation of the entire homeodomain across cell membranes [5]. The pAntp peptide alone retains the membrane translocation properties and has therefore been proposed as a universal intercellular delivery vector [1]. We have recently found that a homologous peptide, pIsl, derived from the Islet-1 homeodomain, also behaves as an efficient CPP [7].

The mechanisms behind the translocation of the CPPs are still mostly unknown, although it is clear that the molecular details of the peptide–membrane interaction are of fundamental importance for the translocation process. The exact role of any secondary structure in the process, though, remains unclear.

Given its helical nature within the homeodomain, as well as the high stability of the helix [8], it was initially assumed that an amphipathic helicity of the pAntp peptide must play a role in the translocation process [9]. This seemed to be supported by the finding that, although largely unstructured when free in aqueous solution, in the presence of SDS micelles or aqueous fluoroalcohol mixtures pAntp adopts an α-helical secondary structure [4,10,11]. Subsequent studies, though, have demonstrated that a helical conformation of a CPP is not mandatory for efficient membrane translocation [5,12].

Phospholipid vesicles provide a more realistic biomembrane model system, convenient for spectroscopic studies. Earlier studies on the secondary structure adopted by pAntp interacting with charged vesicles have shown that it may be helical [13], or have a dominating β-structure [14], depending on the conditions. This is in agreement with an infrared study of the peptide adsorbed on phospholipid monolayers [15]. The β-structure was also found for the pIsl peptide [14]. An analogue of pAntp, with a single proline substitution, was also found to adopt a largely β-structure [5].

The variation of secondary structure of a peptide interacting with a membrane is an interesting problem. The present study was undertaken to examine more closely when these different structures arise. We have used circular dichroism (CD) spectroscopy to characterize the secondary structure induced in pAntp of different concentrations in the presence of phospholipid vesicles of different compositions. We have varied three parameters: surface charge density, lipid-to-peptide molar ratio (L/P), and salt content. Electron paramagnetic resonance (EPR) spectroscopy was used to give information on the binding to vesicles of pAntp, covalently labeled with a spin probe. Intrinsic tryptophan fluorescence was also monitored.

We report that the pAntp peptide exhibits interesting chameleon-like properties at a biomembrane surface. This means that although pAntp does adopt some secondary structure upon binding to a charged phospholipid surface, the structure differs according to the conditions at the membrane. Furthermore, the ability of pAntp to change conformations while bound to a membrane might contribute to the understanding of the translocation mechanism.

2. Materials and methods

2.1. Materials

pAntp and cys(-1)-pAntp were produced by Neosystem Laboratoire, Strasbourg. The identity and purity were ascertained by amino acid, mass spectral and HPLC analysis. 1-Palmitoyl-2-oleoyl-phosphatidylcholine (POPC; Avanti Polar Lipids, Alabaster, USA) and 1-palmitoyl-2-oleoyl-phosphatidylglycerol (POPG; Avanti) were used without further purification. The thiol-specific spin label reagent 1-oxyl-2,2,5,5-tetramethyl-pyrroline-3-methyl) methanethiosulfonate (MTS-SL) was purchased from Renal Factory (Budapest).

2.2. Preparation of vesicles

Vesicles were prepared by initially dissolving the phospholipids at the desired concentration (with the chosen POPG/POPC molar ratio) in chloroform, to ensure the complete mixing of the components, and then removing the solvent by placing the sample in a vacuum for 3 h. The dried lipids were then dissolved in 50 mM potassium phosphate buffer (pH 7.0). In some experiments, the effect of salt was tested by including 150 mM potassium fluoride (KF) in the medium. The ice-cooled dispersion was sonicated, using a Heat System Model 350 A Sonifier, under nitrogen until the sample became transparent. The duration of sonication was approximately 30 min, with the microtip at a low output. Titanium particles from the microtip and lipid debris were removed by centrifugation at $25\,000 \times g$. Ultracentrifugation was also used but did not improve the light scattering properties. This preparation procedure should result in vesicles, the so-called small unilamellar vesicles (SUVs), with dimensions of less than 100 nm in diameter, as determined by earlier spin-label studies [16].

2.3. Determination of peptide concentrations

After weighing on a microbalance, the peptide concentrations in the stock solutions were determined spectrophotometrically. A molar absorptivity of 5600 M^{-1} cm^{-1} for tryptophan was applied.

2.4. Spin-labeling of pAntp

Cysteine-pAntp was dissolved in a mixture of acetonitrile and aqueous 0.1% trifluoroacetic acid, together with an excess of the thiol-specific MTS-SL reagent, as previously described [14]. The product was purified by reversed HPLC on a C18 column with an acetonitrile/trifluoroacetic acid gradient.

2.5. EPR spectroscopy

EPR spectra were recorded on a Bruker Lexus500 spectrometer system, operating at 9.2 GHz, with a rectangular cavity. Each sample was drawn into a flat cell, which was then kept at room temperature (20 °C). Conventional first-derivative spectra were recorded at a modulation frequency of 100 kHz and amplitude of 0.3 mT. The spectra were averaged over 15 scans, with a sampling time of 0.3 s.

2.6. Fluorescence spectroscopy

Tryptophan fluorescence was measured on a Perkin Elmer LS 50B Luminescence Spectrometer with FL WinLab software. All measurements were taken in 4 × 10 mm cuvettes at 20 °C. The fluorescence was excited at 280 nm and the emission scanned from 300 to 500 nm. Scans were taken with 3 nm excitation and emission band widths, at a scan speed of 250 nm/min.

2.7. Monitoring the binding of pAntp to vesicles by fluorescence

Increasing concentrations of pAntp, from a 1 mM stock solution, were added to vesicles with 1 mM phospholipid concentration, produced from POPG/POPC mixtures. The corresponding wavelength of the Trp fluorescence maximum, λ_{em}, was recorded. Each measurement was performed after equilibrium had been reached, and the background signal due to the lipids was subtracted.

2.8. CD spectroscopy

CD measurements were made on a Jasco J-720 CD spectropolarimeter with 0.5 and 1 mm quartz cuvettes. Wavelengths from 190 to 250 nm were measured, with a 0.2 nm step resolution at 100 nm/min speed. The response time was 4 s, with 50 mdeg sensitivity and a 2 nm band width. The temperature was regulated by a PTC-343 controller, set at 20 °C. Spectra were collected and averaged over 40 scans. pAntp, at various concentrations (according to the experiment), was added from a stock solution to vesicles composed of 1 mM phospholipid, with varying compositions. Contributions from background signals were subtracted from the CD spectra acquired for the peptide.

To aid in the interpretation of the CD spectra, computer fitting experiments using the VARSELEC program [17], with five reference component spectra, were performed. Quantitative contributions of spectral components from different secondary structures could be estimated. The program resolves contributions from three β components (antiparallel, parallel and turn). We have combined these to a single β component, in addition to α-helical and random coil components. For a flexible peptide, the estimated percentages of secondary structure components should not be taken as absolute measures, but rather reflect on relative changes between spectra in a series of experiments.

3. Results

3.1. Monitoring the spin labelled cys-pAntp (SL-pAntp) binding to vesicles by EPR

Our earlier reported EPR results [14] demonstrated that no binding of SL-pAntp takes place to neutral PC vesicles. In order to obtain further information about the interaction between pAntp and the vesicles, EPR spectra (in parallel with CD) were recorded of SL-pAntp in the presence of vesicles containing 2–100 mol% POPG. The experiments were performed with both the low and high peptide concentrations in order to compare the degree of peptide binding in both cases. Fig. 1b–f shows spectra recorded with 10 and 80 μM SL-pAntp in the presence of vesicles produced from 1 mM phospholipids, together with a spectrum (Fig. 1a) of 10 μM SL-pAntp free in aqueous solution. The double integrals were evaluated for all spectra in Fig. 1, and were found to be (on a relative scale): (a) 1.00; (b) 1.07; (c) 1.04; (d) 1.04; (e) 1.02; (f) 4.51. The spectra are shown normalized to the same double integral to facilitate comparison of the line-shapes.

With low POPG content in the vesicles, it is apparent that the binding of the peptide is not complete. With 2 mol% POPG, a clear, narrow component from the free, mobile, peptide can be seen at the high field side (Fig. 1b). By resolving the spectra into the two components, free and bound, we estimate that free state represents about 25% of the total population. With 10 mol% POPG, at L/P ~ 100, the EPR spectrum (Fig. 1c) indicates more complete binding, with the narrow component from the free peptide almost disappearing. Here we estimate that the free state is about 5% of the total population.

Above 30 mol% POPG, there is no evidence of any free peptide, and all is bound to the vesicles. In the presence of 1 mM POPG/POPC [30:70], we have recorded spectra for 10 and 80 μM SL-pAntp (Fig. 1d and f, respectively). Although there is no obvious difference in the line shapes, a factor of only 4.5 difference is observed between double integral values reflecting the intensities of the 80 and 10 μM SL-pAntp spectra, instead of the expected factor of 8 due to the different concentrations. All 10 μM peptide samples had double integrals well within the expected experimental uncertainty.

The fact that the EPR spectra were identical at 30 mol% POPG (Fig. 1d) and 100 mol% POPG (Fig. 1e) also indicates that at this L/P there is no apparent change in the mobility of the vesicles themselves, even at such a high lipid charge density. While a basic peptide such as pAntp could possibly fuse/aggregate vesicles of high charge densities, we have no evidence for this under the present

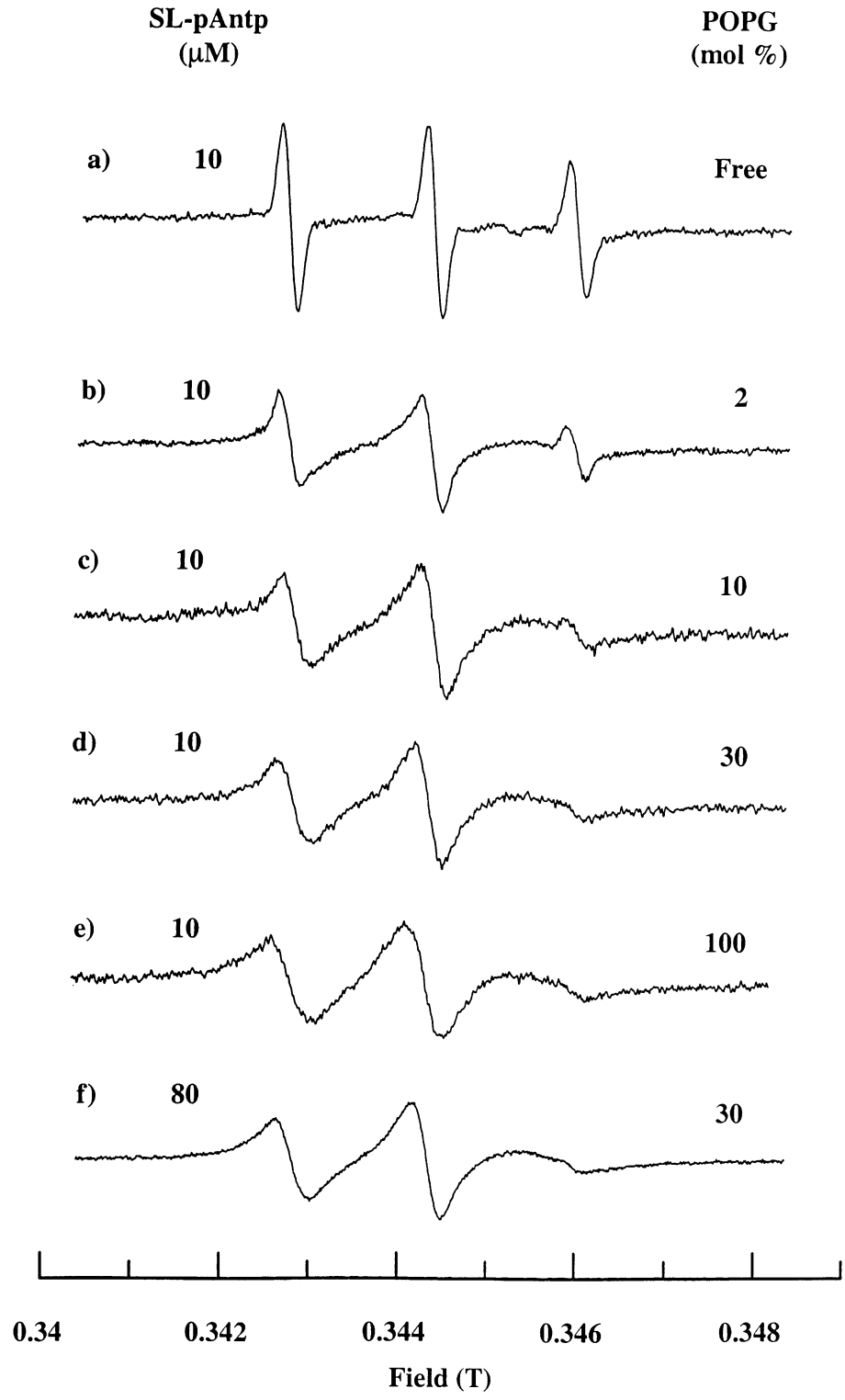

Fig. 1. EPR spectra demonstrating the binding of SL-pAntp to vesicles with different charge densities. The vesicles were produced from 1 mM phospholipids, POPG/POPC, with 2–100 mol% POPG in 50 mM phosphate buffer. The spectra are shown normalized to the same double integral (the relative double integral values of the spectra are given in parentheses). (a) SL-pAntp (10 μM) free in aqueous solution (set to 1). SL-pAntp (10 μM) in the presence of vesicles containing different mol% POPG: (b) 2% (1.07); (c) 10% (1.04); (d) 30% (1.04); (e) 100% (1.02). (f) SL-pAntp (80 μM) in the presence of 30 mol% POPG vesicles (4.51). The spectra were recorded at an ambient temperature (around 20 °C).

conditions. This phenomenon should most likely take place at very low L/Ps, outside the range employed here [18].

There is a small contribution of a very weak and constant signal on the high-field side ($m_I = -1$) in all the EPR spectra. Whether this narrow signal is due to a contamination is not clear. It appears in different synthetic batches after the HPLC purification. The constant nature of this minor component seems to indicate that it is in fact related to the peptide. It may reflect a local N-terminal mobility of the spin label moiety at the membrane interface. We have earlier reported [14] that the overall correlation time estimated for the SL-pAntp probe, even when bound, is faster than expected from the rotation of a particle with the size of a vesicle. The spin label moiety seems to retain considerable local mobility in the vesicles.

3.2. Monitoring pAntp binding to vesicles by fluorescence

The change in the wavelength of Trp fluorescence maximum, λ_{em}, upon binding to phosopholipid vesicles was used to confirm the binding of pAntp to vesicles of different charge densities. Increasing concentrations of pAntp were added to vesicles composed of 1 mM phospholipids with different POPG mol% content. The corresponding λ_{em} was plotted as a function of L/P (Fig. 2).

With neutral (POPC) vesicles, the lack of binding is characterized by an almost constant λ_{em} around 354 nm, at all L/P ratios. This is the emission wavelength for the free peptide [14]. With charged vesicles, binding clearly takes place. At high L/P ratios, the λ_{em} is "blue-shifted" to 339 nm. This corresponds to the wavelength of the peptide fully bound to vesicles [14]. The degree of full binding is maintained down to L/P ~ 12, below which the λ_{em} begins to decrease ("red-shift"). The decreased λ_{em} indicates the presence of nonbound peptide. The free peptide population at L/P ~ 5 (end of titration) is larger the lower the charge density of the vesicle. The observation that all peptide is bound, when L/P ≥ 12 for vesicles with more than 30 mol% POPG content, means that at the L/P range 17–500 where the CD experiments were carried out (see below), there is full binding of the peptide to the vesicles at all times.

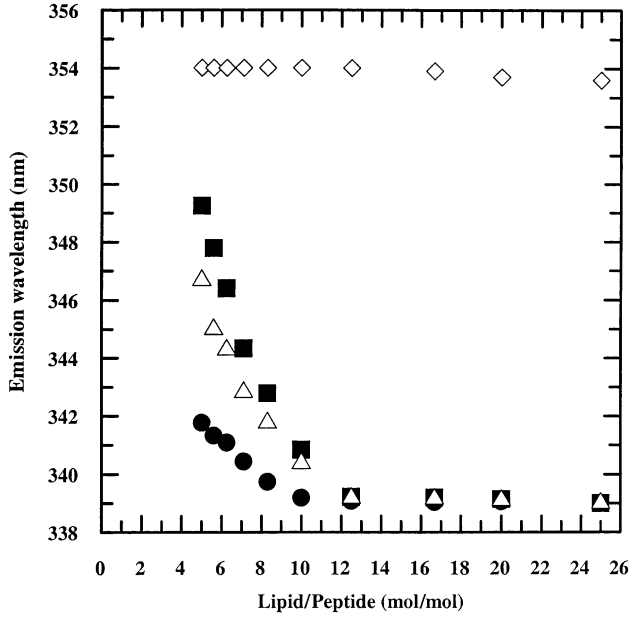

Fig. 2. The wavelength of the Trp fluorescence maximum, λ_{em}, as a function of L/P, upon binding of pAntp to vesicles of different charge densities. Increasing concentrations of pAntp, from a 1 mM stock solution, were added to vesicles composed of 1 mM phospholipid mixtures of different POPG/POPC content. The samples contained vesicles from POPC (◇), POPG/POPC [30:70] (■), POPG/POPC [50:50] (△), or POPG (●). The medium was 50 mM phosphate buffer. The spectra were recorded with a 280 nm excitation wavelength and 3 nm excitation and emission band widths, at an ambient temperature (around 20 °C).

3.3. Monitoring the secondary structures of pAntp by CD

In the present study, we are primarily interested in the conformational states of pAntp bound to phospholipid vesicles, i.e. within the regions defined by the EPR and fluorescence results. pAntp again did not show any interaction with neutral (zwitterionic) vesicles, requiring some (minimum) membrane surface charge density in order to bind (data not shown). The structure induced in pAntp in the presence of vesicles with various POPG/POPC compositions, as well as with different L/P molar ratios, was studied by CD spectroscopy. In addition, the effect of a higher ionic strength was investigated.

3.3.1. The effect of surface charge density

Fig. 3 shows CD spectra of 8 μM pAntp in the presence of 1 mM POPG/POPC vesicles with varying POPG content. Assuming that the two lipid components occupy approximately the same molecular surface area, we, for simplicity, account for the charge density as mol% of POPG of the total lipids. Table 1 summarizes the quantitative evaluation of the spectra in terms of three secondary structure components: α-helix, β-structure and random coil. From the CD spectra (Fig. 3 and Table 1), we observe that increasing the vesicle charge density leads to an α- to β-structure conformational transformation. When free in aqueous solution, pAntp has a low propensity for a helical structure. A random coil state dominates, but there is also a fairly large β-structure content present (Table 1). With neutral POPC vesicles, no structure induction takes place relative to the state in aqueous solution (data not shown), in agreement with our earlier observations with different phosphatidylcholine vesicles [14]. With only 2% charge density on the vesicle, the EPR results show that pAntp is only partially bound. With 10% charge density, most of the pAntp is bound according to the EPR results. The CD spectrum shows a mixture of structural states, with an increased helical content. Increasing the charge density to 20%, a biologically relevant situation, the pAntp becomes completely bound and adopts a fairly high, maximal, α-helix content (around 60%). As the charge density is increased further, the helix content decreases and, instead,

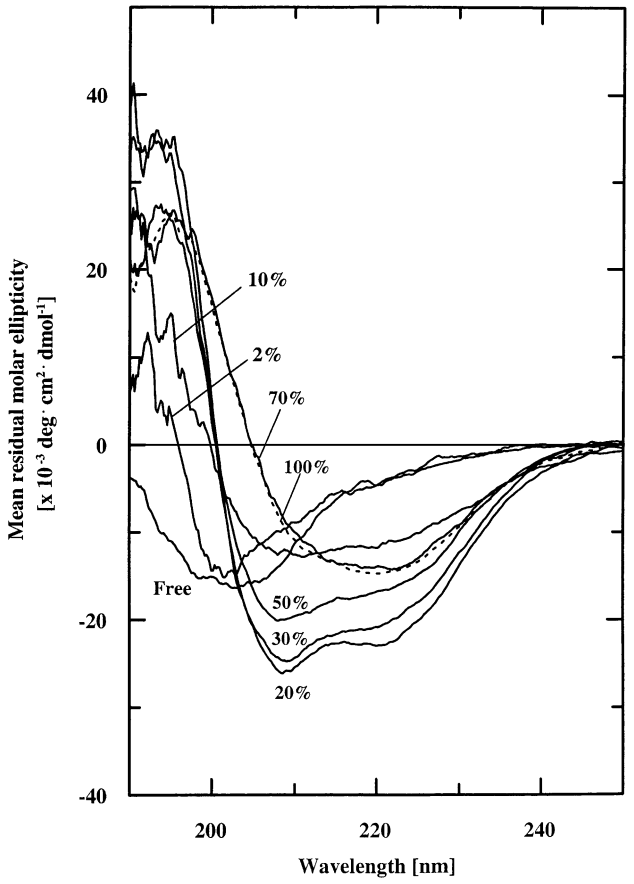

Fig. 3. Surface charge density induced conformational change in the pAntp. The CD spectra show 8 μM pAntp in the presence of 1 mM phospholipid (POPG/POPC) vesicles with increasing POPG content (2–100 mol%). The medium used was 50 mM potassium phosphate buffer, KP_i (pH 7.0). The temperature was set at 20 °C.

a concurrent increase in β-structure is observed. At the given lipid-to-pAntp ratio (L/P ~ 125), the β-structure content increases with the POPG molar fraction, but in the range 70–100% POPG, the CD spectra become insensitive to the variation in the surface charge. At this high surface charge density, there is around 50% β-structure, at maximum.

Table 1
Surface charge density (mol% POPG) induced conformational states in the pAntp peptide in the presence of phospholipid vesicles of varying composition

POPG (mol%)	α-helix (%)	β-structure (%)	Random (%)
Free	16	26	57
2	21	28	50
10	34	19	46
20	65	20	15
30	61	25	14
50	53	35	12
70	30	51	18
100	31	49	19

Shown are the values from the decomposition of conformational components of the CD spectra in Fig. 3. The values were obtained by computer fittings using the VARSELEC program [17]. The concentration of pAntp was 8 μM in the presence of vesicles from 1 mM POPG/POPC, corresponding to an L/P molar ratio of 125. The vesicles have a variable mol% POPG content, in the range 2–100%. The medium was 50 mM potassium phosphate buffer (pH 7.0). The temperature was set at 20 °C.

3.3.2. The effect of the pAntp concentration

Fig. 4 shows the CD spectra with increasing pAntp concentrations (2–60 μM) in the presence of POPG/POPC vesicles at a 30:70 molar ratio. The total lipid concentration is 1 mM, and the titration covers the L/P range of 17–500. Corresponding quantitative estimations of secondary structure contributions are summarized in Table 2. Again, we observe an $\alpha \rightarrow \beta$ transformation in this series of experiments due to increasing peptide concentrations. At low pAntp concentrations of around 2 μM, corresponding to L/P ~ 500, the α-helix content is at a maximum. Increasing the pAntp concentration leads to a gradual decrease in this helicity, and an increase in the β-structure content of the pAntp. The maximum β-structure content is observed at the highest pAntp concentration of 60 μM, where L/P ~ 17.

Fig. 5 shows the CD spectra with an increasing pAntp concentrations (2–60 μM) in the presence of 1 mM POPG, i.e. 100% charged vesicles. Table 3 gives the quantitative

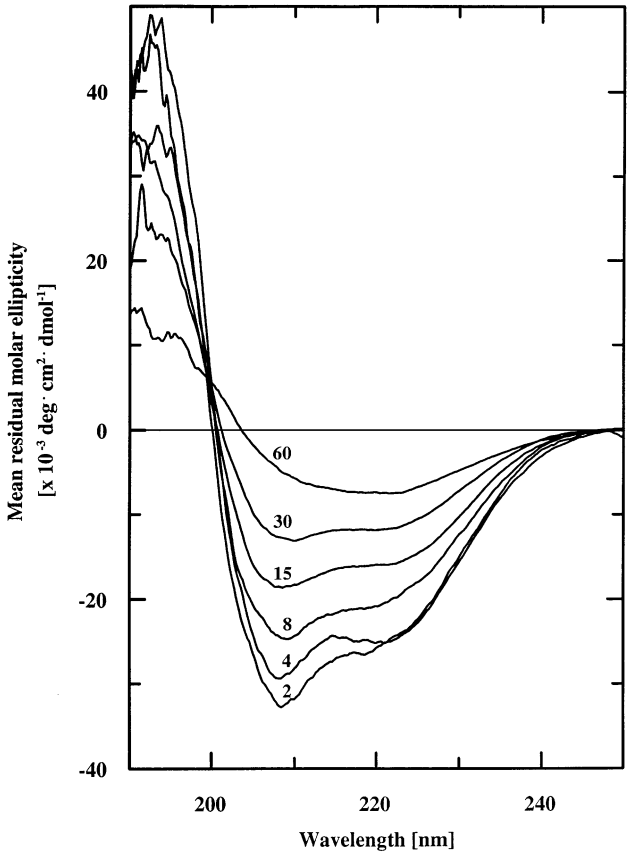

Fig. 4. L/P ratio induced conformational change in the pAntp. The CD spectra show 1 mM POPG/POPC [30:70] vesicles titrated with increasing concentrations of pAntp (2–60 μM); 50 mM phosphate buffer (pH 7.0) medium.

Table 2
Changes in the conformational states of pAntp bound to phospholipid vesicles, induced by variation of the L/P molar ratio

pAntp concentration (μM)	L/P	α-helix (%)	β-structure (%)	Random (%)
2	500	69	18	13
4	250	67	17	15
8	125	61	25	14
15	67	48	33	17
30	33	35	42	22
60	17	18	57	24

The structural components of the CD spectra in Fig. 4 were obtained by computer fittings [17]. Vesicles from 1 mM POPG/POPC [30:70], i.e. with 30 mol% POPG, were titrated with pAntp (2–60 μM). Fifty millimolar phosphate buffer (pH 7.0) was used as medium.

evaluation of secondary structures. Here the same trend is observed as with the 30% charged vesicles. An $\alpha \rightarrow \beta$ transformation still takes place. However, the highest helix content, induced at the highest L/P ~ 500 (2 μM pAntp), is lower (54%, Table 3) than that induced with POPG/POPC [30:70] vesicles (69%, Table 2). On the other hand, the maximal β-like content, which is obtained at the lowest L/P, is the approximately the same for both lipid charge densities.

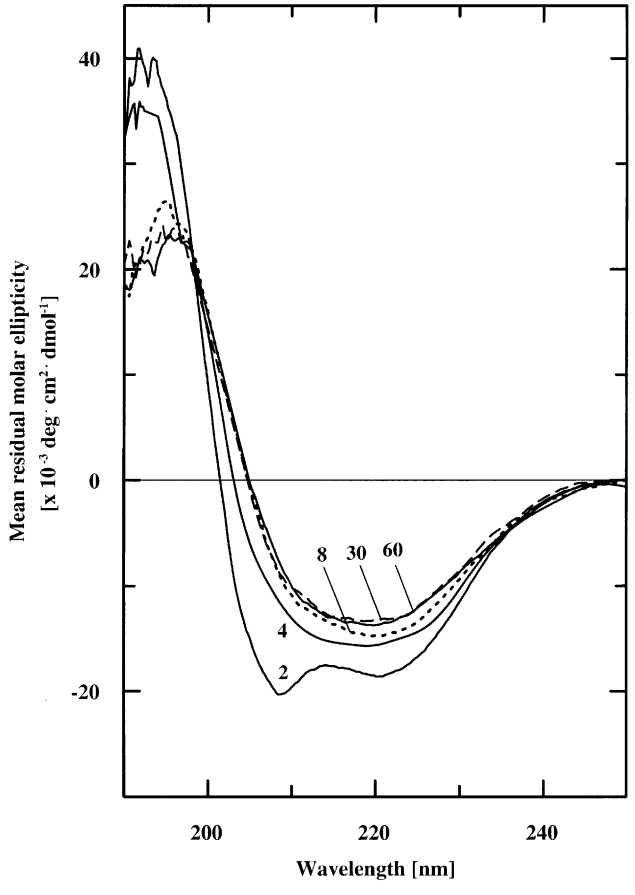

Fig. 5. L/P ratio induced conformational change in the pAntp. The CD spectra show 1 mM POPG vesicles titrated with increasing concentrations of pAntp (2–60 μM); 50 mM phosphate buffer (pH 7.0) medium.

Table 3
L/P ratio induced conformational change in the pAntp peptide bound to phospholipid vesicles, at two different salt concentrations

pAntp concentration (μM)	L/P	α-helix (%)		β-structure (%)		Random (%)	
		50 mM KP_i	+150 mM KF	50 mM KP_i	+150 mM KF	50 mM KP_i	+150 mM KF
2	500	54	63	31	25	15	12
4	250	40	60	38	24	22	15
8	125	31	58	49	32	19	10
30	33	28	34	54	46	18	19
60	17	29	26	53	51	17	23

The table shows a decomposition of the conformational components of the CD spectra (Figs. 5 and 6) of 1 mM POPG (100%) vesicles titrated with increasing concentrations of pAntp (2–60 μM). The samples contained 50 mM potassium phosphate, KP_i (pH 7.0), as such (Fig. 5), or with extra 150 mM potassium fluoride, KF (Fig. 6).

3.3.3. Samples at a higher salt concentration

The effect of electrostatic contributions to the induced structures was investigated by raising the ionic strength above that of the standard buffer. One hundred percent POPG vesicles were produced both in the standard buffer (50 mM potassium phosphate), and with an added 150 mM KF. We again varied the L/P ratio, this time in the samples containing 150 mM KF, by titration with pAntp. The binding of the pAntp was confirmed by its tryptophan fluorescence. The maximum emission wavelength at 339 nm, characteristic of completely bound pAntp [14], remained unchanged under all conditions included here (data not shown). Fig. 6 shows CD spectra from 100% POPG vesicles with the added salt in the L/P range 17–500. Fig. 6 (inset) also shows, for comparison, the situation at L/P = 125 with 100% POPG vesicles at the two ionic media. Table 3 includes the quantitative evaluations of the secondary structures of the CD spectra in Fig. 6. Compared to fully charged vesicles in the standard buffer, the addition of 150 mM KF gives a higher contribution of pAntp in an α-helical state, at the expense of the β-state, for the lower peptide concentrations ($L/P \geq 33$). The effect of salt becomes insignificant only at the highest peptide concentrations.

Fig. 7 illustrates the induction of α-helix as a function of L/P as reflected in the change in CD intensity at 208 nm (θ_{208}), from Figs. 4–6. At this wavelength, the α-helix ellipticity has a maximal value, whereas the random coil and β-structure values are low (or even constant if an isodichroic situation prevails). The two lipid charge densities of the vesicles are compared: POPG/POPC [30:70] and 100% POPG, the latter at the two ionic strengths. The increasing ellipticities at 208 nm, and hence the α-helix contributions, are generally compensated for by decreased β-structure contributions, since the random coil contributions are approximately invariant (10–20%) under the conditions

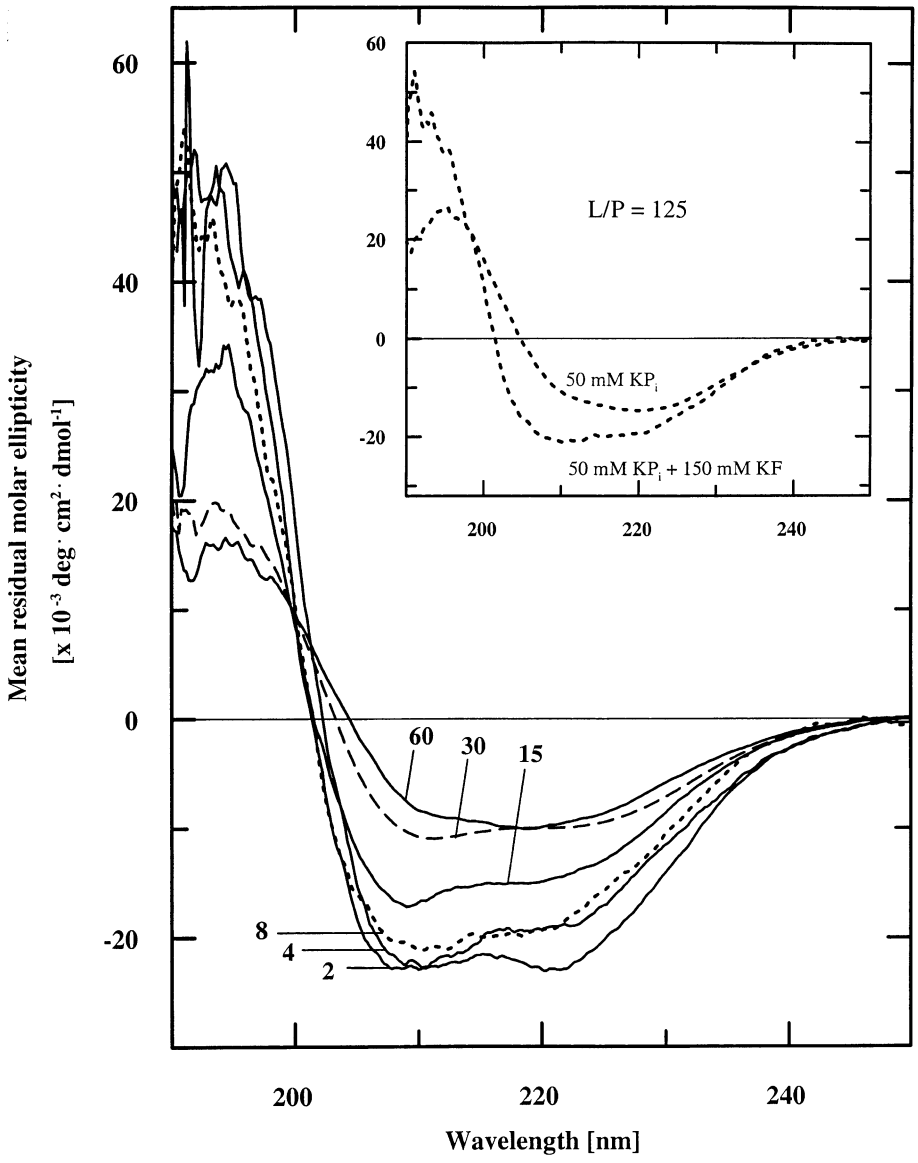

Fig. 6. L/P ratio induced conformational change in the pAntp, with a high salt medium. The CD spectra show 1 mM POPG vesicles titrated with increasing concentrations of pAntp (2–60 μM); 50 mM phosphate buffer (pH 7.0) plus 150 mM potassium fluoride, KF. Inset: A comparison between the two CD spectra at L/P = 125 (· · ·), with and without (Fig. 5) the extra potassium fluoride (KF).

applied. Hence, the increasing ellipticities with increasing L/P ratio depicted in Fig. 7 demonstrate a $\beta \rightarrow \alpha$ transition in the peptide, under conditions where EPR and fluorescence results show that the peptide is completely bound to the vesicle. For the POPG/POPC [30:70] vesicles in 50 mM KP_i the β-structure → α-helix transition starts at the lowest L/P of 17, and proceeds abruptly up to L/P ≈ 125. After that, the transition levels out at a ratio of L/P ≈ 500, where the α-content has its maximum value (69%, Table 2). For the pure POPG vesicles, there is a small plateau at low L/P, followed by a slow and gradual increase in the α-helix content up to L/P ≈ 500. At this ratio, the ellipticity induced by the POPG vesicles is equivalent to around only half of that induced by the POPG/POPC [30:70] vesicles. On the other hand, the ellipticity value for the POPG vesicles at the lowest L/P value (12.5) is only slightly higher than that with the POPG/POPC [30:70] vesicles. At the higher ionic strength medium, the variation of the CD θ_{208} value shows a strong dependence on the L/P, with the 100% POPG vesicles, even at low ratios, and the $\beta \rightarrow \alpha$ conformational change becomes more prominent.

These results indicate that the nature of the induced structure in the pAntp peptide is highly dependent on its environment, in a rather complex manner. Surface charge density of the vesicles, salt concentration and L/P ratio are all critical variables. The optimum conditions for α-helix induction in pAntp appear to be a high L/P, coupled with a low surface charge. On the other hand, the optimum con-

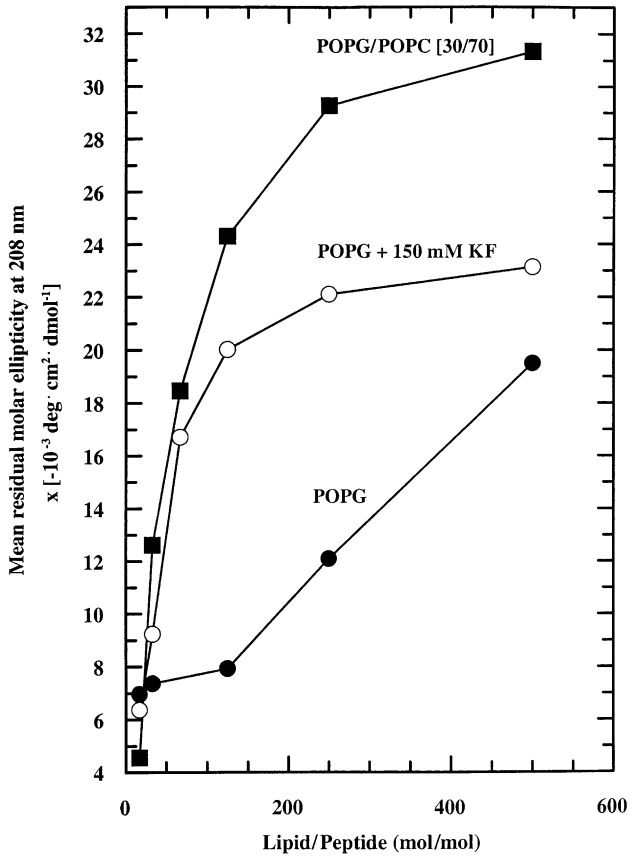

Fig. 7. Negative ellipticity value measured at 208 nm, θ_{208}, as a function of the molar L/P ratio, obtained by adding increasing concentrations of pAntp, in two different media. The values are obtained from Figs. 4–6. The samples contained vesicles from 1 mM POPG (●, ○), or 1 mM POPG/POPC [30:70] (■). The medium was either 50 mM phosphate buffer (●, ■), or 50 mM phosphate buffer plus 150 mM potassium fluoride (○).

ditions for β-structure induction in the pAntp appear to be a low L/P value, coupled with a high membrane charge density or low ionic strength.

4. Discussion

In common with other CPPs, pAntp contains several basic, positively charged amino acids. The seven charged residues in pAntp are distributed all over the molecule, with only a few hydrophobic residues in between. This makes pAntp relatively water soluble. When free in an aqueous solution, pAntp adopts predominantly a random coil, but there also exists a rather large contribution from a β-structure state (Table 1). We have not seen any evidence for (oligomeric) peptide aggregation, reflected in the CD properties for pAntp in aqueous solution, even at concentrations up to 1 mM (data not shown). In addition to the charged amino acids, certain hydrophobic acids also contribute to the membrane binding and translocation. The tryptophans, in particular the one at position 48, have been suggested to be crucial for effective translocation [4,5,19,20].

Due to its poor amphipathicity, coupled with a relatively low hydrophobicity, pAntp requires negative surface charge density on the membrane in order to interact. In investigations of the importance of membrane electrostatics to peptide binding and secondary structure induction, it is common in the literature to use fully (100%) charged vesicles, produced from various acidic phospholipids. This was also the approach in our earlier study [14], where we employed dimyristoyl- and dioleoyl-phosphatidylglycerol vesicles. In another study of pAntp, Drin et al. [13] used small vesicles produced from POPG/POPC with a 30:70 molar ratio. They reported the helical content to be 47%, with L/P = 325, and Tris-buffered saline. This sample had a quite high total lipid concentration (16 mM). We were not able to record high-quality CD spectra from such lipid samples due to light scattering problems around 200 nm. Hence, in our CD study [14], we restricted the total phospholipid concentration to 0.1–1 mM. In this concentration range, resulting in values for L/P ≤ 100, we derived a dominating β-structure (sheet) component, in addition to a random coil state.

The binding of pAntp to the vesicles was independently monitored by EPR spectroscopy on a spin-labeled peptide, and by fluorescence spectroscopy using the intrinsic tryptophan fluorescence. We have taken care to ensure conditions in which a high degree of binding to the vesicles prevails. We observed by EPR that a few mol% (< 10%) POPG is not enough for effective pAntp binding to the vesicles, even at L/P ~ 100. Full pAntp binding was achieved at L/P ≥ 12 by having around 20–30% charge density. This may be an optimal composition for vesicles as a model system for biological membranes and more relevant than vesicles composed of fully charged lipids alone.

Under conditions of complete binding of pAntp to the vesicles, we observed that pAntp undergoes interesting conformational changes. The results obtained in this study suggest that the secondary structure of pAntp depends on two main factors: (1) electrostatics, and (2) the peptide surface occupancy. The first factor includes variables influencing the surface potential, such as the surface charge density and the ionic strength. The second factor is influenced by the L/P ratio, under conditions of complete binding. In order to vary the L/P ratio, we have preferred to fix the value of the lipid concentration at 1 mM, and instead vary the peptide concentration. This method has allowed us to still record good CD spectra even at L/P ~ 500.

At a given L/P value, a lower surface charge density promotes a higher degree of helicity within pAntp. However, as the charge density is increased over a critical value, a reduction in the helical content and an increase in the β-structure content is observed (Fig. 3). There is no indication of a simple two-state conversion since no evidence for an isodichroic point is seen. The β-structure content maximizes

at >70% surface charge density, when L/P ~ 125, and 50 mM phosphate buffer is used as medium.

The same trend was observed by varying the L/P ratio using vesicles with two different charge densities, 30% and 100% (Figs. 4–6). In both cases, it was observed that at higher L/P ratios (i.e. low peptide concentration), pAntp adopts a more α-helical structure, while at lower L/P, it adopts a higher degree of β-structure. However, it is apparent that at the low charge density, the tendency to form an α-helix is stronger than at the high charge density (Fig. 7). Moreover, with the low surface charge density (30%) sample, the conversion between the α- and β-states seems not to involve any other states, since there is clear isodichroic point at around 200 nm (Fig. 4).

The transition from the α-helix state (Fig. 1d) to the β-structure state is facilitated either by an increase in the peptide concentration (Fig. 1f), or an increase in the mol% POPG (Fig. 1e). The importance of the L/P ratio for the $\alpha \rightarrow \beta$ conversion (Fig. 4) suggests that peptide–peptide interaction or aggregation at the vesicle may be correlated with the induction of β-structure. The estimated intensities of the EPR spectra, comparing 10 and 80 μM concentrations of SL-pAntp in the presence of 1 mM POPG/POPC [30:70] vesicles, may also be understood in this context. Although not obviously different in line-shape, the double integral of the EPR spectrum of the 80 μM SL-pAntp is about a factor of 2 lower than expected from the eight-fold increase in concentration. This effect may in fact be due to spin–spin interactions between aggregated SL-pAntp on the membrane surface. It has been shown in an early study on interacting spins in a rigid lattice [21] that dipolar coupling between interacting spins may lead to a situation where a diminished "normal" radical spectrum is seen on top of an "unobservable" severely broadened spectrum. Although the "rigid-lattice" approximation is not strictly valid for the spin-labeled pAntp interacting with the vesicle, a similar mechanism, though less effective, may be operating here.

The dependence of β-structure on the vesicle surface charge density may also be explained by peptide aggregation. The higher negative charge density may be more effective in neutralizing the electrostatic repulsion between the positively charged peptides, hence facilitating interactions between them.

In agreement with the suggestions put forward in Refs. [15,22], our preliminary studies with fluorescence quenching and polarization indicates that the pAntp molecules lie on the membrane surface with both the tryptophans partly exposed to the solvent, irrespective of the surface charge of the vesicles (data not shown).

A higher surface charge density will create a stronger surface potential. The pAntp is highly charged and requires only a relatively small potential to become electrostatically attached. The effect of salt (ionic strength) is primarily to screen this potential. Raising the ionic strength will then have a similar effect to lowering the surface charge density. We could see that the addition of a monovalent salt (KF) promoted a weakening of the β-state and a stabilization of the α-state. The two conformational states seem to be able to coexist at the membrane surface. Interfacial phenomena can often be satisfactorily treated by a Poisson–Bolzmann theory. However, in the pAntp case, the binding isotherm may reflect the secondary structure variations. Hence, we do not know, for instance, whether specific bindings, like salt bridges, between the basic residues of the pAntp and lipid head groups are required.

The secondary structure conversion observed here is not restricted to pAntp, and we have, so far, come across two related reports on peptide–membrane interactions, where the peptides undergo an $\alpha \rightarrow \beta$ transition. The first case deals with a synthetic ion channel forming model peptide, $(LARL)_3(LRAL)_3$, which has no structure in water [23]. It contains almost the same number of charged residues as pAntp, but is more hydrophobic and amphipathic. It therefore also binds to neutral vesicles, forming an α-helix. In the presence of vesicles containing 25% charged lipids, this peptide forms a β-structure. Upon addition of NaCl to the acidic vesicles, a conformational transition takes place in the peptide from the β-structure to the α-helix state. The authors propose that these conformational transitions may facilitate the initiation process of the channel formation by this peptide in the lipid bilayer. The second report of interest deals with the Aβ(1–40) peptide, related to the Alzheimer's disease [24]. This peptide undergoes a random coil to β-structure transition upon binding to charged vesicles at low L/P value. When increasing the L/P value, this β-structure state converts into an α-helical state. The conversion was followed by CD where the Aβ peptide, at a fixed concentration, was titrated with vesicles containing either 100% POPG or POPG/POPC [25:75].

Although the translocation of CPPs takes place within many biological cells, it is not obvious that this is also the case in a membrane model system. A similar fluorescence technique as used with real cells was applied by Thorén et al. [25], who observe an uptake of pAntp into giant membrane vesicles, produced from soybean phospholipids. This finding is contrasted by the recent reports by Drin et al. [13,20], where all the pAntp remained at the outer surface of smaller vesicles. However, besides the vesicle size, there is another difference in the conditions between the two studies, namely in the L/P ratio. While Thorén et al. [25] employ a low L/P of around 46, in the case of Drin et al. [13], the L/P is 325. From the current study, we know that the two L/P values may give rise to two different conformational states of pAntp. This means that translocation was observed under conditions where more β-structure is expected, while no such translocation was reported to take place in conditions favoring the α-state.

The observed secondary structures of pAntp may be viewed in the context of some of the translocation models that currently exist. One model that we can discard is that of pore-formation. In agreement with the observed low-lytic behavior of pAntp in cellular systems [1,2], no leakage was

observed for the peptide in model studies, down to L/P ~ 10 (where the peptide adopts a β-structure) [25]. This indicates that pAntp does not form pores in the manner of certain antimicrobial peptides [26].

An early model, based on membrane model experiments, suggested the so-called inverted micelle formation in the bilayer [11]. In this model, pAntp (with a cargo) perturbs the membrane and becomes accommodated within an aqueous cavity, and then transiently internalized. Such a mechanism should minimize leakage, but it is difficult to see how a relatively large cargo can be accommodated.

An alternative that we favor is the ''membrane-thinning'' model, as suggested for magainin 2 [27]. In this model, initially the peptides, in their monomeric state, carpet the membrane, causing an electrostatic perturbation in the outer leaflet. This results in a lateral rearrangement of the (acidic) lipids, and a thinning of the membrane takes place. At this point, it is possible that the peptides interact (or aggregate) on the surface, and the reduced local surface tension would allow the CPPs to intercalate the membrane. Flexible sealing between peptide side-groups and lipid head-groups will minimize leakage until the CPPs slip through onto intracellular targets. This transient permeation is followed by a rapid healing of the membrane.

The exact role of any secondary structure of pAntp, transient or not, and its relation to aggregation during the translocation process is still a problem for further studies. In this study, we have demonstrated that pAntp can undergo an $\alpha \rightarrow \beta$ transition depending on experimental conditions in a simple model system. We conclude that the pAntp CPP has revealed an interesting phenomenon in terms of being a structural ''chameleon'' in its adaptation to the membrane environment, and we expect other peptides also to possess this property.

Acknowledgements

We would like to thank Mr. Torbjörn Astlind for expert instrumental assistance and Dr. Jüri Jarvet for valuable help with the CD spectral analysis. This study was supported by grants from the Swedish Natural Science Research Council and from the EU program contract No. MAS3-CT97-0156.

References

[1] D. Derossi, G. Chassaing, A. Prochiantz, Trends Cell Biol. 8 (1998) 84–87.
[2] M. Lindgren, M. Hällbrink, A. Prochiantz, Ü. Langel, Trends Pharmacol. Sci. 21 (2000) 99–103.
[3] A. Prochiantz, Hum. Psychopharmacol. 14 (1999) S11–S15.
[4] D. Derossi, A.H. Joliot, G. Chassaing, A. Prochiantz, J. Biol. Chem. 269 (1994) 10444–10450.
[5] D. Derossi, S. Calvet, A. Trembleau, A. Brunissen, G. Chassaing, A. Prochiantz, J. Biol. Chem. 271 (1996) 18188–18193.
[6] A. Prochiantz, Ann. N. Y. Acad. Sci. 886 (1999) 172–179.
[7] K. Kilk, M. Magzoub, M. Pooga, L.E.G. Eriksson, Ü. Langel, A. Gräslund, Bioconjugate Chem. 12 (2001) 911–916.
[8] U. Mayor, C.M. Johnson, V. Dagett, A.R. Fersht, Proc. Natl. Acad. Sci. U. S. A. 97 (2000) 13518–13522.
[9] A. Prochiantz, Curr. Opin. Neurobiol. 6 (1996) 629–634.
[10] M. Lindberg, A. Gräslund, FEBS Lett. 497 (2001) 39–44.
[11] J.-P. Berlose, O. Convert, D. Derossi, A. Brunissen, G. Chassaing, Eur. J. Biochem. 242 (1996) 372–386.
[12] A. Scheller, B. Wiesner, M. Melzig, M. Bienert, J. Oehlke, Eur. J. Biochem. 267 (2000) 6043–6049.
[13] G. Drin, H. Déméné, J. Temsamani, R. Brasseur, Biochemistry 40 (2001) 1824–1834.
[14] M. Magzoub, K. Kilk, L.E.G. Eriksson, Ü. Langel, A. Gräslund, Biochim. Biophys. Acta 1516 (2001) 77–89.
[15] E. Bellet-Amalric, D. Blaudez, B. Desbat, F. Graner, F. Gauthier, A. Renault, Biochim. Biophys. Acta 1467 (2000) 131–143.
[16] B.M. Backlund, G. Wikander, T. Peeters, A. Gräslund, Biochim. Biophys. Acta 1190 (1994) 337–344.
[17] P. Manavalan, W.C. Johnson Jr., Anal. Biochem. 167 (1987) 76–85.
[18] D. Persson, P. Thorén, B. Nordén, FEBS Lett. 505 (2001) 307–312.
[19] P.M. Fischer, N.Z. Zhelev, S. Wang, J.E. Melville, R. Fåhraeus, D.P. Lane, J. Pept. Res. 55 (2000) 163–172.
[20] G. Drin, M. Mazel, P. Clair, D. Mathieu, M. Kaczorek, J. Temsamani, Eur. J. Biochem. 268 (2001) 1304–1314.
[21] J.S. Leigh, J. Chem. Phys. 52 (1970) 2608–2612.
[22] G. Fragneto, F. Graner, T. Charitat, P. Dubos, E. Bellet-Amalric, Langmuir 16 (2000) 4581–4588.
[23] S. Lee, T. Iwata, H. Oyagi, H. Aoyagi, M. Ohno, K. Anzai, Y. Kirino, G. Sugihara, Biochim. Biophys. Acta 1151 (1993) 76–82.
[24] E. Terzi, G. Hölzemann, J. Seelig, Biochemistry 36 (1997) 14845–14852.
[25] P. Thorén, D. Persson, M. Karlsson, B. Nordén, FEBS Lett. 482 (2000) 265–268.
[26] M. Zasloff, Nature 415 (2002) 389–395.
[27] S. Ludtke, K. He, H. Huang, Biochemistry 34 (1995) 16764–16769.